УДК 621.391: 621.396: 621.373
https://doi.org/10.32362/2500-316X-2026-14-2-57-68
EDN XPSWYV

RESEARCH ARTICLE

Generation of radiovision signals by spectral saturation in transient distortion mode of integral microwave amplifiers for gesture recognition systems

Kirill V. Latyshev [@], Mihail S. Kostin, Konstantin A. Boikov

MIREA – Russian Technological University, Moscow, 119454 Russia
[@] Corresponding author, e-mail: latyshev@mirea.ru

• **Submitted:** 17.06.2025 • **Revised:** 29.09.2025 • **Accepted:** 09.02.2026

Abstract

Objectives. The paper aims to investigate the mechanisms of the nonlinear formation of a wideband pulse spectrum under overload conditions in ultra-wideband (UWB) amplifier circuits in resolving problems related to radiovision gesture recognition. The relevance of the study stems from the need to enhance the accuracy and noise immunity of modern radiovision UWB systems for gestural control interfaces.

Methods. The study used statistical radiophysics, time-frequency methods of wavelet transformation of radio images, the theory of *S*-parametric vector analysis of circuits, and software-numerical modeling.

Results. The method for generating UWB signals in the microwave range based on controlled nonlinear signal distortion is presented. When the amplifier is switched to the saturation mode, a signal with sharp fronts is formed with a wide energy spectrum. A laboratory setup of a cyber-physical system for gesture recognition using radio sensing was developed, and its characteristics were investigated. The properties of the pulses generated in radiovision control systems were also studied. The effectiveness of the proposed approach for the tasks of radiovision gesture recognition was experimentally demonstrated.

Conclusions. A method of nonlinear saturation-synthesis of the spectrum of radiovision signals based on transient distortion phenomena in UWB amplifiers is proposed. It was shown that, when the initial frequency band is expanded up to 900 MHz, the interference mode can provide phase image repeatability of at least 0.94. It was also established that in the input overloaded mode of the SBB5089Z[1] type amplifier with low-mode harmonic excitation at a transition frequency of 47 MHz in a cascade amplification scheme, a signal with a modified spectrum can be obtained at the output of the radio antenna. In this case, the controlled formation of the antenna excitation spectrum for each amplifier module is determined by means of the unique impulse characteristic of the integrated UWB-amplifier. This allows for the successful application such amplifiers in resolving problems related to radiovision gesture recognition. The methodology proposed allows the use of standard UWB amplifiers to create compact sources of UWB signals without the complication of circuitry.

Keywords: radiovision signal, spectrum saturation, transient distortion, ultra-wideband amplifier, gesture recognition, cyber-physical stand

[1] High-linearity wideband, monolithic microwave integrated circuit (MMIC) amplifier was developed by Qorvo, USA.

For citation: Latyshev K.V., Kostin M.S., Boikov K.A. Generation of radiovision signals by spectral saturation in transient distortion mode of integral microwave amplifiers for gesture recognition systems. *Russian Technological Journal.* 2026;14(2):57–68. https://doi.org/10.32362/2500-316X-2026-14-2-57-68, https://www.elibrary.ru/XPSWYV

Financial disclosure: The authors have no financial or proprietary interest in any material or method mentioned.

The authors declare no conflicts of interest.

НАУЧНАЯ СТАТЬЯ

Формирование радиовизионных сигналов спектральной сатурацией в режиме переходных искажений интегральных сверхвысокочастотных усилителей для систем распознавания жестов

К.В. Латышев [@], М.С. Костин, К.А. Бойков

МИРЭА – Российский технологический университет, Москва, 119454 Россия
[@] Автор для переписки, e-mail: latyshev@mirea.ru

• **Поступила:** 17.06.2025 • **Доработана:** 29.09.2025 • **Принята к опубликованию:** 09.02.2026

Резюме

Цели. Цель работы – исследование механизмов нелинейного формирования широкополосного импульсного спектра в условиях перегрузки в сверхширокополосных (СШП) усилительных цепях для решения задач радиовизионного распознавания жестов. Актуальность исследования обусловлена необходимостью повышения точности и помехоустойчивости современных радиовизионных СШП-систем для жестикулярных интерфейсов управления.

Методы. Использованы методы статистической радиофизики, частотно-временные методы вейвлет-преобразования радиоизображений, методы теории S-параметрического векторного анализа схем, методы программно-численного моделирования.

Результаты. Представлен метод генерации СШП-сигналов в сверхвысокочастотном диапазоне, основанный на управляемых нелинейных искажениях сигнала. Показано, что при переводе усилителя в режим насыщения формируется сигнал с резкими фронтами, обладающий широким энергетическим спектром. Построен лабораторный стенд киберфизической интерференционной радиосенсорной системы распознавания жестов и исследованы его характеристики. Исследованы свойства полученных импульсов в задачах радиовизионного управления. Экспериментально показана эффективность предложенного метода для задач радиовизионного распознавания жестов.

Выводы. Предложен метод нелинейной сатурации – синтеза спектра радиовизионных сигналов, основанный на явлениях переходных искажений в СШП-усилителях. Показано, что интерференционный режим при расширении исходной полосы частот до 900 МГц способен обеспечить повторяемость фазовых изображений не менее 0.94. Установлено, что в перегруженном по входу режиме усилителя типа SBB5089Z[2] при задающем низкомодовом гармоническом возбуждении на переходной частоте 47 МГц в каскадной схеме усиления на выходе радиовизионной антенны удается получить сигнал с измененным спектром. При этом управляемое формирование спектра возбуждения антенны для каждого из усилительных модулей определяется уникальной импульсной

[2] Высоколинейный широкополосный монолитный (monolithic microwave integrated circuit – монолитная микроволновая интегральная схема) усилитель, разработанный компанией Qorvo, США. [High-linearity wideband, monolithic microwave integrated circuit (MMIC) amplifier was developed by Qorvo, USA.]

характеристикой интегрального СШП-усилителя. Это позволило успешно применить такие усилители при решении задач радиовизионного распознавания жестов. Предложенная методика позволяет использовать стандартные СШП-усилители для создания компактных источников СШП-сигналов без усложнения схемотехники.

Ключевые слова: радиовизионный сигнал, сатурация спектра, переходные искажения, сверхширокополосный усилитель, идентификация жестов, киберфизический стенд

Для цитирования: Латышев К.В., Костин М.С., Бойков К.А. Формирование радиовизионных сигналов спектральной сатурацией в режиме переходных искажений интегральных сверхвысокочастотных усилителей для систем распознавания жестов. *Russian Technological Journal*. 2026;14(2):57–68. https://doi.org/10.32362/2500-316X-2026-14-2-57-68, https://www.elibrary.ru/XPSWYV

Прозрачность финансовой деятельности: Авторы не имеют финансовой заинтересованности в представленных материалах или методах.

Авторы заявляют об отсутствии конфликта интересов.

INTRODUCTION

Radio sensor systems for close-range cyber-physical monitoring are used to dynamically identify human gestures in areas such as smart medicine, industrial automation and virtual/augmented reality. The high level of reliability and resolution requirements necessitate new methods of forming and processing radio signals [1, 2], making this research highly relevant.

The paper offers a novel approach to the spectral synthesis of such systems. Rather than using traditional high-voltage shapers, it employs an ultra-wideband (UWB) amplifier which operates in deliberate overload mode. In this mode, the amplifier acts as a nonlinear synthesizer, using transient nonlinear distortions (usually considered an undesirable effect) to expand the signal spectrum (spectral saturation). The novelty of this research lies in the deliberate use of these nonlinear effects for controlled spectrum expansion.

The saturation mechanism is due to the amplifier output transistors operating in saturation mode. In this case, the input signal is converted into an almost rectangular pulse shape with very sharp edges. This ensures the synthesis of a wideband spectrum, used in UWB systems [3, 4]. Spectrum expansion increases the resolution of the radio sensor system and improves its resistance to narrowband interference and the accuracy of temporal and spatial gesture localization.

This paper presents theoretical, modeling, and experimental studies of this method of nonlinear spectrum transformation for gesture recognition using radiovision techniques.

2. MODEL OF WIDEBAND SPECTRUM SYNTHESIS OF RADIOVISION SIGNALS BASED ON THE OCCURRENCE OF TRANSITIONAL DISTORTIONS IN UWB AMPLIFIER

The nonlinear formation of the radiovision signal spectrum occurs when UWB amplifier stages operate in overload mode due to transient distortions. These distortions are analytically described in [5] when the equivalent circuit of an UWB stage with inductive correction is analyzed (Fig. 1).

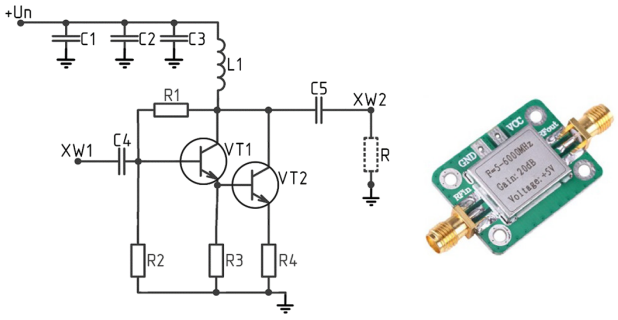

(a) (b)

Fig. 1. SBB5089Z UWB amplifier[3] with inductive correction: (a) schematic diagram; (b) external appearance. The symbols used to denote the circuit elements correspond to those used in GOST 2.710-81[4]

The paper describes the use of a monolithic SBB5089Z-type UWB amplifier, based on InGaP HBT[5] transistors. It uses a Darlington configuration with an active bias circuit.

When the input low-mode signal is formed, the UWB amplifier operates in deliberate overload mode. The L1 inductor with inductance L in the output circuit prevents a rapid increase in current through the load resistor R, equivalent to the input resistance R of the subsequent cascade. This results in a temporary accumulation of energy in the parasitic capacitances of the cascade (the equivalent capacitance C), and the capacitance of the printed circuit board. This slows down transient processes in the initial phase of the signal. As energy accumulates in the L1 inductor, the equivalent capacitance C charges to a voltage level which exceeds

[3] High-linearity wideband, monolithic microwave integrated circuit (MMIC) amplifier was developed by Qorvo, USA.

[4] GOST 2.710-81. Interstate Standard. *Unified system for design documentation. Alpha-numerical designations in electrical diagrams*. Moscow: Izd. Standartov; 1985 (in Russ.).

[5] InGaP is indium gallium phosphide and HBT is a heterojunction bipolar transistor.

the opening threshold of the VT1–VT2 composite transistor cascade. Consequently, the transistors abruptly switch to saturation mode, forming a pulse with steep fronts and a wide spectrum. This is a necessary condition for generating UWB signals.

The signal gain coefficient can be represented in operator form as follows [5]:

$$K(p) = S\frac{(pL+R)\frac{1}{pC}}{pL+R+\frac{1}{pC}} = S\frac{pL+R}{1+pRC+p^2LC},$$

wherein p is the Laplace operator and S is the steepness of the composite Darlington transistor cascade.

Let $K_0 = SR$ be the gain at low frequencies. The time constant of the equivalent circuit is $\tau_{bas} = RC$, and $m = L/CR^2 = (L/R)/CR$ is the correction parameter. Then,

$$\frac{K(p)}{K_0} = \frac{1+p\tau_{bas}m}{1+p\tau_{bas}+p^2m\tau_{bas}^2} = \\ = \frac{1}{\tau_{bas}}\cdot\frac{p+\frac{1}{m\tau_{bas}}}{p^2+\frac{1}{m\tau_{bas}}p+\frac{1}{m\tau_{bas}^2}}.$$

Therefore, the operational signal at the output of the UWB cascade with inductive correction in input overload mode can be represented as follows [5]:

$$\frac{U(p)}{K_0} = \frac{1}{\tau_{bas}}\cdot\frac{p+\frac{1}{m\tau_{bas}}}{p\left(p^2+\frac{1}{m\tau_{bas}}p+\frac{1}{m\tau_{bas}^2}\right)}.$$

The behavior of the transient process is determined by the roots of the characteristic equation of the system, which are calculated using the following formula [5]:

$$p_{1,2} = -\frac{1}{2m\tau_{bas}} \pm \frac{1}{2m\tau_{bas}}\sqrt{4m-1}.$$

When $m > 0.25$, corresponding to the condition for transient oscillations forming with discharge in the transition frequency range when the VT1–VT2 composite cascade is opened instantly, as shown in Fig. 2a, the normalized transfer function of the UWB amplifier is as follows [5]:

$$\frac{h(t)}{K_0} = 1-\frac{2m}{\sqrt{4m-1}}e^{-\frac{t}{2m\tau_{bas}}}\sin\left(\frac{\sqrt{4m-1}}{2m\tau_{bas}}t+\theta\right),$$

wherein $\theta = \pi - \arcsin\frac{\sqrt{4m-1}}{2m}$, and t is time.

In this case, the transition process represents damped oscillations with an emission the magnitude of which depends on the correction coefficient m.

When $m = 1$ (Fig. 2b), which is the condition of free oscillations at the output of the UWB amplifier, the expression for the transfer function is as follows [5]:

$$\frac{h(t)}{K_0} = 1-e^{-\frac{t}{2RC}}\left(\cos\left(\frac{\sqrt{3}t}{2RC}\right)+\frac{1}{\sqrt{3}}\sin\left(\frac{\sqrt{3}t}{2RC}\right)\right).$$

Thus, a transition process corresponding to free oscillations is formed within the transition frequency range of the UWB amplifier's transfer characteristic, which can be modeled as a second-order active bandpass filter.

During time ζ, when $f_1 > f_2$, the system completes a cycle of free oscillations (Fig. 2a), resulting in the formation of a damped radio pulse at the output of the UWB amplifier. This pulse is then amplified by an identical cascade. In this case, the radio pulse exhibits exponential attenuation and is formed in accordance with the system's impulse response. The selection of the low-mode excitation frequency f_1, which corresponds to the transition frequency range, is determined by the conditions necessary to achieve the correction parameter $m = 1$. The frequency f_2 corresponds to linear signal amplification.

It should be noted that overload of the UWB amplifier input at a certain frequency may satisfy the Barkhausen self-excitation condition [6]:

$$|A\beta| \geq 1 \text{ and } \angle A\beta = 2\pi n,\ n \in \mathbb{Z}, \quad (1)$$

wherein A is the gain coefficient, β is the feedback transfer coefficient, $\angle A\beta$ is the phase shift between the input and output through the feedback circuit, and $\mathbb{Z}$ is a set of integers.

Thus, for self-oscillation to occur, the gain must compensate for losses in the feedback circuit and the total phase shift in the circuit must be a multiple of 2π [6].

Let the UWB amplifier have a complex transfer function f, defined as

$$A(f) = \frac{A_0}{1+j\frac{f}{f_c}}, \quad (2)$$

wherein A_0 is the gain at low frequencies, ($f \ll f_c$), f_c is the amplifier cutoff bandwidth, and the following complex feedback function:

$$B(f) = \frac{1}{1+j\frac{f}{f_{band}}}, \quad (3)$$

wherein f_{band} is the feedback circuit band [7].

Taking into account (2) and (3), the loop gain is then:

$$T(f) = A(f)B(f) = \frac{A_0}{\left(1+j\frac{f}{f_c}\right)\left(1+j\frac{f}{f_{band}}\right)}. \quad (4)$$

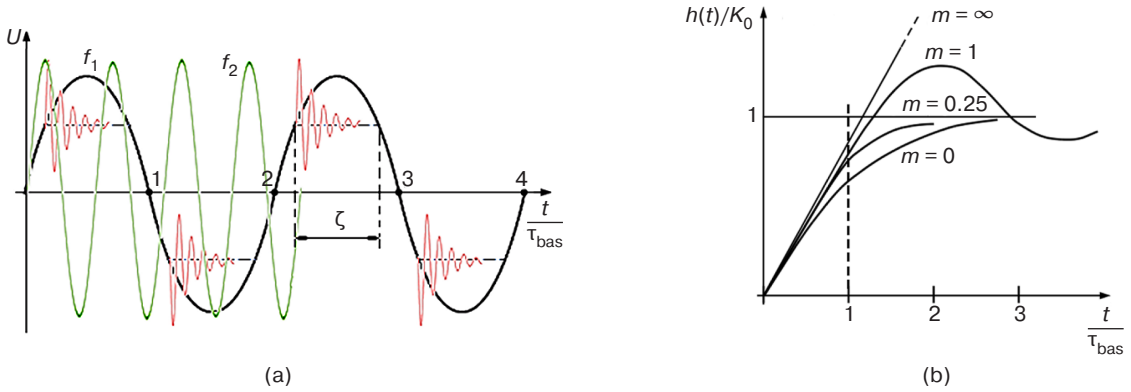

(a) (b)

Fig. 2. Transient distortions at the output of the UWB amplifier:
(a) signal distortions in overload mode within the transition frequency range (normalized values on the X and Y axes);
(b) transfer function of the UWB amplifier for various correction parameter values, *m*

In nonlinear systems, the gain of an amplifier operating in limiting mode is a function of the input signal amplitude V:

$$A(V) = \begin{cases} A_{\text{lin}}, V < V_{\text{sat}}, \\ \dfrac{V_{\text{sat}}}{V}, V \geq V_{\text{sat}}, \end{cases} \quad (5)$$

wherein A_{lin} is the linear value of the gain coefficient and V_{sat} is the amplifier's saturation voltage [8, 9].

The gain declines as $\frac{1}{V}$, when $V > V_{\text{sat}}$. If the feedback circuit transfer coefficient is frequency-dependent, then considering (1) and (3) gives us:

$$|T(f, V)| = |A(f, V)| \cdot B(f) \geq 1. \quad (6)$$

According to Barkhausen's criterion (6), the condition for amplifier self-excitation can only be fulfilled at certain frequencies where the feedback circuit transfer coefficient $B(f)$ reaches significant values. This is possible in the presence of frequency resonance, caused by the corrective (parasitic) inductances and capacitances of the circuit. The physical principle behind this phenomenon is as follows: when an UWB amplifier is operating in a nonlinear signal-limiting (saturation) mode, the output voltage waveform is significantly distorted. It is thus converted from a sinusoidal signal to a signal which is close to a rectangular pulse with sharp fronts and tails. These time variations carry a wide range of high-frequency harmonics, as follows from Fourier transform theory. If these harmonics coincide with the resonant frequencies of the corrective (parasitic) LC[6] chains, the corresponding harmonics are amplified due to an increase in the transmission coefficient $B(f)$. Consequently, the system switches to wideband signal generation mode. In the time domain, this is a damped oscillatory pulse close in shape to a Gaussian monocycle. In the frequency domain, it has a wide energy spectrum band which covers a range of up to hundreds of megahertz [8, 10–12].

Let us consider the process of exciting a radiovision antenna with a synthesized radio pulse. The electric component of the radiovision signal field ($E(t)$) at the output of the UWB antenna is known to be proportional to the derivative of the excitation signal current function:

$$E(t) \approx \frac{dI_{\text{вых}}(t)}{dt} h_A(t),$$

wherein $I_{\text{out}}(t)$ is the excitation radio pulse current formed at the output of the UWB amplifier cascades with a certain pulse characteristic, $h_A(t)$ [13].

In order to create a numerical model of the synthesis of radiovision signals based on cascades of UWB amplifiers, experimental measurements of *S*-parameters were performed on a sample of three randomly selected SBB5089Z UWB amplifiers. The *S*-parameters of the UWB amplifier line were recorded using an R&S ZNLE[7] vector network analyzer in the 0.01–5 GHz frequency band (Table 1).

Table 1. Radio technical characteristics of UWB amplifiers

Parameter	SBB5089Z	TQP7M9103[8]	WYDZ[9]
Gain, dB	20–30	30	60
Passband, MHz	50–6000	10–3000	1–2000
Noise level, dB	3.5	4	6–8
Maximum output power, dBm	23	20	15
Maximum input power, dBm	15	10	5

[6] An electrical circuit consisting of an inductor (L) and a capacitor (C) connected together.

[7] R&S ZNLE is a vector network analyzer manufactured by Rohde & Schwarz, Germany. It is designed for testing high-frequency electronic components such as filters, amplifiers, cables, and antennas.

[8] TQP7M9103 is a high-power signal amplifier manufactured by Qorvo, USA.

[9] WYDZ is a low-noise amplifier manufactured by TZT, China.

Based on the vector measurement results shown in Fig. 3, the S_{21} transfer characteristics were converted into vector arrays for the interpretation of UWB amplifiers during the software-numerical simulation of a radiovision signal generator in the *MATLAB Simulink*[10] environment (Fig. 4).

The synthesized excitation spectrum generator circuit of the UWB antenna consists of the following functional blocks: *1* is a low-mode signal generator with frequency selection corresponding to $m = 1$; *2* is a radio system input parameters block specified by a special Simscape library which determines the main characteristics of the signal transmitted to the UWB amplification path; *3* is UWB amplifier for forming transient distortions; *4* is an amplifier for further signal transmission (the S_{21} transfer characteristics are loaded from the arrays obtained from the vector measurements); *5* is a radio system output parameters block; *6* is an oscilloscope which records the UWB antenna excitation signal; and *7* is a radio system properties block which defines global simulation parameters such as frequency range, noise, impedance, etc.

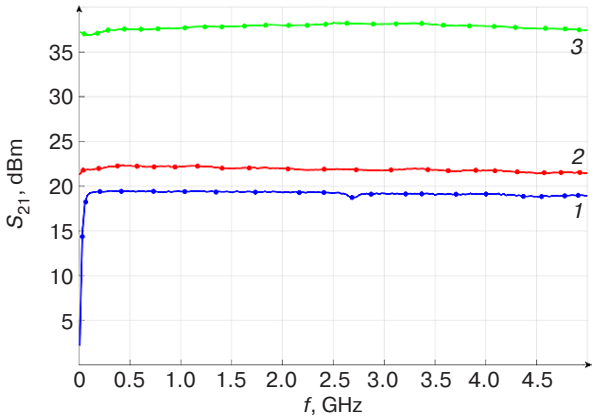

Fig. 3. Transfer characteristics of S_{21} UWB amplifiers: SBB5089Z (*1*), TQP7M9103 (*2*), and WYDZ (*3*)

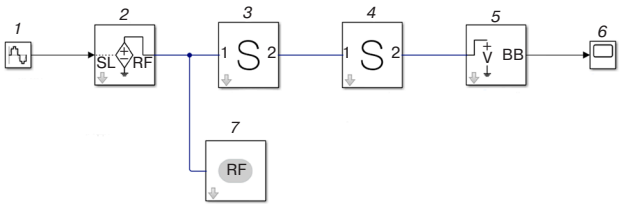

Fig. 4. A model of a nonlinear synthesizer for the radiovision excitation signal spectrum of a UWB antenna. RF stands for radio frequency, SL for *Simulink*, which receives a signal from a standard *Simulink* block, and BB for baseband

The equivalent circuit of a second-order RLC[11] filter (Fig. 5) can be used to represent an amplifying UWB cascade with inductive correction (Fig. 1). When a step input is applied to the circuit (which is equivalent to the sudden opening of a transistor in saturation mode), the transient process is governed entirely by the correction parameter *m*. Therefore, the objective is to select operating conditions for the amplifier such that $m = 1$.

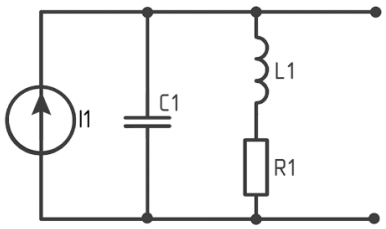

Fig. 5. Equivalent circuit of a second-order RLC filter

The parameters R1, L1, and C1 in the equivalent circuit are not constant values. Rather, they represent the effective parameters of the amplifier which depend on the frequency of the input signal. Consequently, the correction parameter *m* itself is a frequency-dependent function, $m(f)$. The objective is to determine the optimal excitation frequency, f_{opt}, at which $m(f_{opt}) = 1$ is satisfied.

Analysis of the parameters (Fig. 3) of the SBB5089Z amplifier reveals a 40–50 MHz range where the amplitude-frequency characteristic exhibits an anomaly, indicating complex interactions between internal reactive elements. This region corresponds to the zone in which the amplifier is susceptible to oscillatory transient processes. Modeling in *Simulink* (Fig. 4) has shown that excitation at a frequency of 47 MHz and input overload (amplitude 400 mV) results in a mode corresponding to $m = 1$. The simulated pulse signal of the excitation function, characterized by low-mode oscillation, is shown in Fig. 6.

After passing through the amplification path, overload at the input of the first UWB amplifier in transient mode results in a synthesized signal with an extended spectrum at the output of the second UWB amplification cascade. This exhibits nonlinear spectral saturation in the 0–900 MHz band. Considering the impulse response of the Vivaldi-type strip slot UWB antenna used in this study, the *E* radiovision signal spectrum at its output is shown in Fig. 7.

Signal spectrum conversion analysis was performed during simulation in the *MATLAB Simulink* environment. The original harmonic signal with a frequency of 47 MHz has a narrowband spectrum. The effective spectrum width of the initial signal, calculated at −10 dB from

[10] https://www.mathworks.com/products/simulink.html. Accessed February 06, 2026.

[11] An electrical circuit consisting of a resistor (R), an inductor (L) and a capacitor (C).

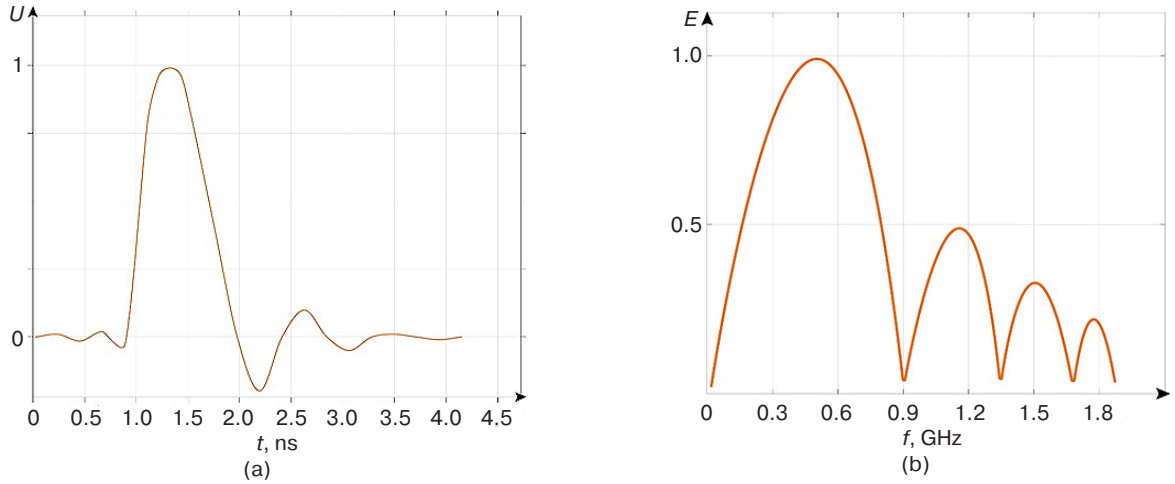

Fig. 6. Pulse excitation signal synthesized by a low-mode oscillation UWB antenna in the overloaded dynamic mode of the SBB5089Z UWB amplifier (normalized values on the vertical axes):
(a) time representation of the radio pulse *U*;
(b) spectrum *E* synthesized from the transient distortions of the radio pulse

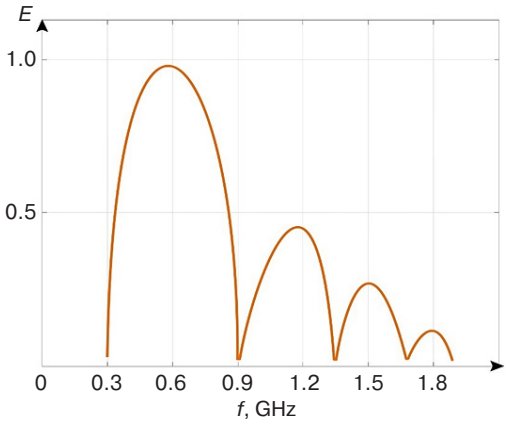

Fig. 7. Spectrum of the radiovision signal at the output of the Vivaldi UWB antenna (normalized values on the *E* axis)

peak power, is ~42.25 MHz. After passing through the proposed amplification system operating in intentional overload and controlled transient distortion mode, the signal undergoes nonlinear spectral transformation. A short radio pulse with steep fronts, characteristic of UWB signals, is formed at the system output. Analysis of the output signal shows that its effective spectral width has expanded to ~900 MHz (also at −10 dB), corresponding to a spectral expansion factor of more than 20.

2. RECOGNITION OF RADIOVISION IMAGES OF GESTURES FORMED IN RESPONSE TO A SYNTHESIZED RADIOVISION SIGNAL

The experimental part of the study aimed to verify the effectiveness of nonlinear formation of the radiovision signal spectrum and to confirm the results of numerical modeling. The effectiveness of identification systems is largely determined by the characteristics of the probing signal, so this approach was chosen. The width of the spectrum and the pulse shape directly affect the resolution, noise immunity, and reliability of feature extraction. The aim of the experiment was to identify four different hand gestures and evaluate the accuracy, stability, and reliability of the recognition system.

In order to conduct experiments based on the model of a nonlinear synthesizer of the radiovision signal excitation spectrum of an SSP antenna (Fig. 4), a cyber-physical stand for identifying hand gestures (Fig. 8) was created. This stand consists of the following blocks:

- R&S SMBV100B[12] vector pulse generator designed to generate the initial harmonic signal. Using the data obtained in the first part of the article, the signal is generated at a frequency of 47 MHz;
- an UWB signal generation block consisting of two low-noise SBB5089Z UWB amplifiers operating in a deliberately overloaded mode (Fig. 3);
- an antenna system comprising a pair of Deepace R101C[13] Vivaldi-type UWB transceiver antennas which emit a probing signal (Fig. 7) and receive the reflected response from the object (hand);
- a received signal amplification unit consisting of two UWB signal amplifiers;

[12] SMBV100B is a high-performance vector signal generator manufactured by Rehde & Schwarz, Germany. It is designed to generate complex and modulated radio frequency (RF) signals for testing and measuring purposes.

[13] Deepace R101C is an ultra-wideband, directional antenna manufactured by Deepace, China. It is used for the reception and transmission of high-frequency signals over a wide range of frequencies.

- data acquisition system consisting of an R&S RTO2032[14] digital oscilloscope to digitize and record the received signals;
- a processing unit consisting of a personal computer with specialized software for processing, analyzing, and visualizing the data received.

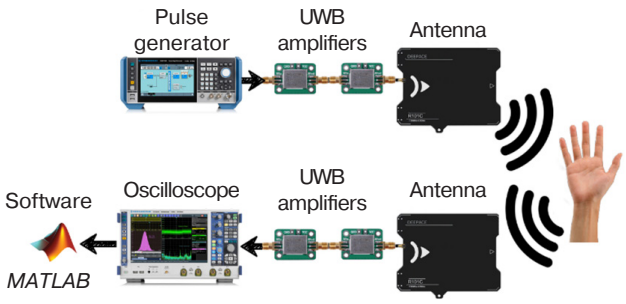

Fig. 8. Cyber-physical stand for identifying hand gestures

The experiment involves the following gestures: rotating the wrist (rotation), pushing the wrist away from the chest (pushing), swiping from right to left (swiping), and clenching the fist (clenching), as shown in Fig. 9. These movements cover a wide range of characteristics of gesture kinematics, providing variety in terms of direction and type of movement [14–16]. They are simple and easy for humans to understand, and are widely used in everyday life for controlling digital devices [17]. The choice of gestures is also dictated by their functional significance in interfaces (Table 2).

Each gesture is represented by a set of ten control frames, combined into a single final radio image or "reference radio portrait" which uniquely identifies the gesture in question (Fig. 10). During the experiment, correlation coefficients are calculated to analyze the linear relationship between the selected gestures. The results of the experiment demonstrate the high level of accuracy of the identification system in recognizing repeated gestures, as indicated by intra-group correlation values close to 1. The coefficients are 0.95 for hand rotation, 0.99 for repulsion, 0.96 for fist clenching, and 0.97 for swiping (Table 3). These results confirm the stability of the system in recognizing the same movements.

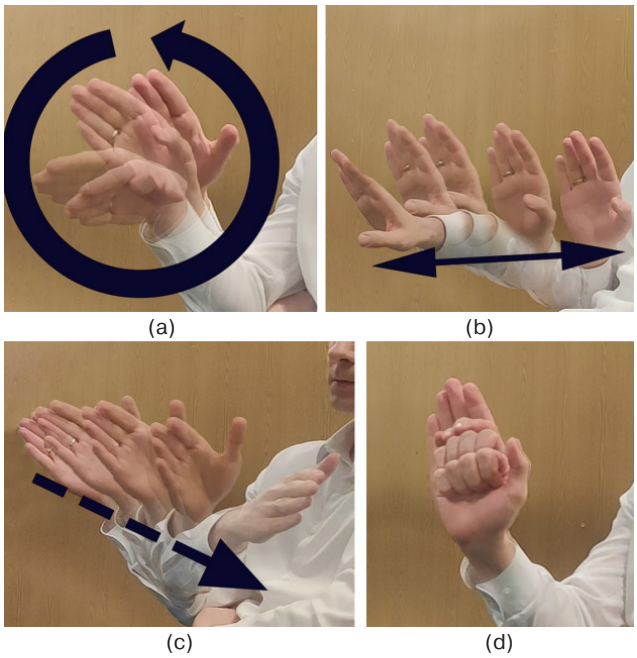

Fig. 9. Gestures used in the experiment: (a) rotation; (b) pushing; (c) swiping; (d) clenching

Table 2. Gesture characteristics

Characteristics / Gesture	Type of movement	Amplitude, cm	Gesture duration, s	Kinematic characteristics	Functionality in the interface
Rotation	Continuous and periodic	<15	0.4	Changing the angle of the hand in relation to the signal direction	Managing settings, scrolling settings
Pushing	Forward	>30	0.8	Movement from the center of the body	Cancel/Dismiss
Swiping	Horizontal	15–30	0.6	Clearly defined direction	Navigating the interface
Clenching	Static	<5	0.3	Altering the hand shape without significantly moving it	Confirming or activating commands

[14] R&S RTO2032 is a digital oscilloscope designed for analyzing complex signals in a variety of fields. It is manufactured by Rehde & Schwarz, Germany.

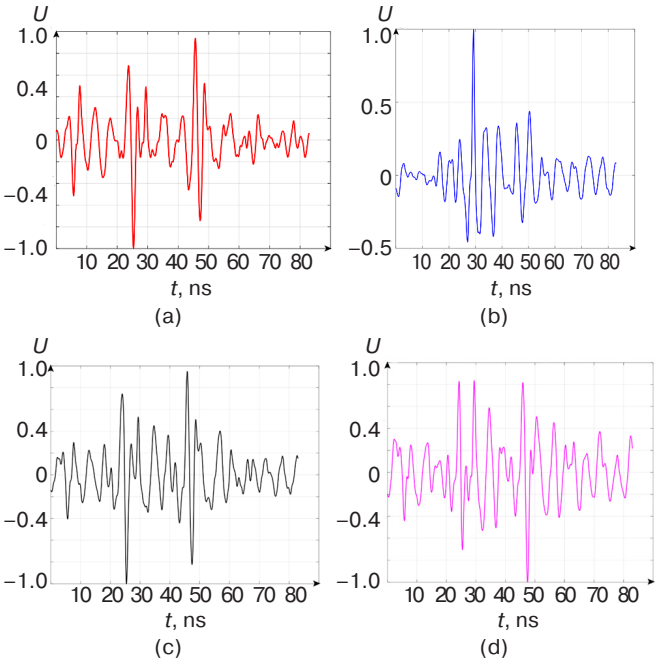

Fig. 10. Representation of reference radio gesture images (normalized values along the vertical axis): (a) rotation, (b) pushing, (c) clenching, and (d) swiping

Certain pairs of gestures exhibit a strong correlation, for instance, clenching a fist and swiping, with a value of 0.84. This suggests a similarity in the signs utilized by the system for their recognition. Conversely, rotation and swiping exhibit an average correlation of 0.62 which could be attributed to the shared elements of hand movement. Furthermore, a moderate relationship exists between pushing and swiping, with a score of 0.65. This can be explained by the directional aspect inherent to both motions.

A low correlation is observed between rotation and pushing (0.30), as well as between pushing and clenching (0.48). These motions have significantly different kinetic characteristics, indicating that they can be easily distinguished by the system.

Based on the findings, it can be inferred that the system successfully recognizes the selected gestures with a high level of accuracy and reliability. This is attributed to the consistent and reproducible UWB pulse waveform obtained when the SBB5089Z amplifier is activated.

The experiment also studied the response of the gesture recognition system to erroneous or missing control frames of a gesture. In order to evaluate the system's tolerance for error, the number of distorted or skipped frames was consistently increased from one to nine. The findings indicate that different gestures exhibit varying degrees of resilience to incorrect (missing) frames (Fig. 11). Specifically, the push-off gesture demonstrated the greatest stability, whereas the swipe gesture exhibited the least. These results suggest that successful gesture recognition necessitates a different number of control frames for each gesture.

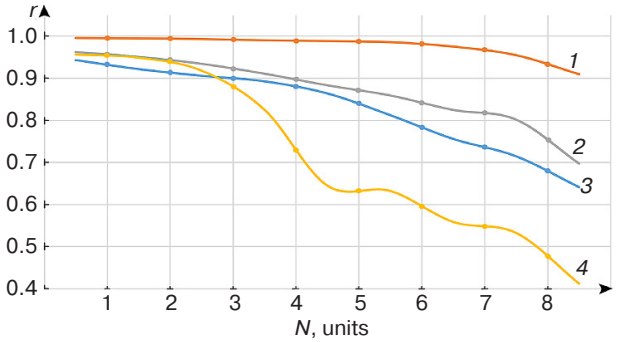

Fig. 11. Impact of the number *N* of incorrect gesture frames on the correlation coefficient *r* with the reference image: *1* is pushing; *2* is clenching, *3* is rotation; and *4* is swiping

The experiment demonstrates that the recognition system achieves a correlation coefficient of over 0.95 for gesture recognition. However, its resistance to false negatives (missed frames) varies depending on the specific gesture. Repulsion and compression gestures

Table 3. Average correlation coefficient between reference radio portraits and performed gestures

Gesture \ Reference radio portrait	Rotation	Pushing	Clenching	Swiping
Rotation	**0.95**	0.30	0.82	0.62
Pushing	0.30	**0.99**	0.48	0.65
Clenching	0.82	0.48	**0.96**	0.84
Swiping	0.62	0.65	0.84	**0.97**

Table 4. Evaluation of experiment repeatability

Gesture	Number of gestures performed	Number of correctly recognized gestures	Repeatability
Rotation	100	95	0.95
Pushing		98	0.98
Swiping		96	0.96
Clenching		94	0.94

are more robust, achieving a correlation coefficient of over 0.90 with up to four missed frames. These gestures are therefore suitable for use in challenging conditions where data may be incomplete or distorted due to interference or reduced recording quality. In contrast, swiping with a brush requires more stringent quality control, since it relies on the accuracy of the entire image sequence.

The results highlight the need to analyze each gesture in detail when developing recognition systems. Gestures which are highly sensitive to distortion, such as swiping, may require additional optimization of data processing algorithms or the incorporation of error compensation mechanisms. This would improve the reliability of the system in real-world environments, where data loss or partial corruption is inevitable.

An experiment was also conducted to assess the repeatability of gesture identification. Each gesture was repeated 100 times and the identification results were analyzed (Table 4).

Based on the results, it can be inferred that the recognition accuracy has consistently exceeded 0.94. Considering this level, the experiment can be regarded as reliable. The impact of random factors is negligible and the findings can be confidently applied in practice.

CONCLUSIONS

1. The S-parameters of three UWB radio-frequency amplifiers were determined and analyzed. As a result, it was found that the SBB5089Z UWB has the ability to control signal distortion within the range of 40–50 MHz, in order to expand the output spectrum. The correction parameter was determined to be 1 at 47 MHz.
2. A method for the nonlinear synthesis of a radio imaging signal spectrum was proposed, enabling a spectrum expansion coefficient value of over 20 to be achieved.
3. The proposed gesture recognition system based on the proposed method demonstrated a high level of accuracy. The correlation coefficients between the recognized gestures and their corresponding fiducial gestures are 0.99 for the repulsive gesture, 0.95 for the rotation gesture, 0.96 for the scrolling gesture, and 0.96 for the compression gesture.
4. Particular attention was paid to system resilience to erroneous or missing frames influencing the gesture recognition process. System response to partial data loss within each gesture was also investigated. The findings show that all gestures can be recognized with a correlation coefficient of over 0.9.
5. The repeatability of gesture recognition is at least 0.94.

Authors' contributions

K.V. Latyshev—developing the software-numerical model and laboratory stand of a cyber-physical monitoring system for radio-frequency identification of human gestures.

M.S. Kostin, K.A. Boikov—developing the nonlinear synthesized spectrum of a radiovision signal under overloaded ultra-wideband amplification mode.

REFERENCES

1. Khan I., Kwon Y. Radar-based Hand Gesture Recognition with Feature Fusion using Robust CNN-LSTM and Attention Architecture. *IEEE Access*. 2025;13:69281–69291. https://doi.org/10.1109/ACCESS.2025.3558293
2. Kostin M.S., Boikov K.A. Digital technologies for signal radio vision and radio monitoring. *Russian Technological Journal*. 2024;12(4):59–69. https://doi.org/10.32362/2500-316X-2024-12-4-59-69
3. Wu M. Gesture Recognition Based on Deep Learning: A Review. *EAI Endorsed Transactions on e-Learning*. 2024;10. https://doi.org/10.4108/eetel.5191
4. Qu C., Zhang Y., Jin L., et al. Exploring hand gesture recognition using micro-Doppler radar data based on vision transformers. *J. Phys.: Conf Ser*. 2023;2504:012046. https://doi.org/10.1088/1742-6596/2504/1/012046

5. Sedra A., Smith K., Carusone T., Gaudet V. *Microelectronic Circuits* (*The Oxford Series in Electrical and Computer Engineering*). 8th ed. Oxford University Press; 2020. P. 58–134, 174–246, 508–696.
6. He F., Ribas R., Lahuec C., Jézéquel M. Discussion on the general oscillation startup condition and the Barkhausen criterion. *Analog Integr. Circ. Signal Process*. 2009;59:215–221. https://doi.org/10.1007/S10470-008-9250-1
7. Razavi B. *RF Microelectronics* (*Prentice Hall Communications Engineering and Emerging Technologies Series*). 2nd ed. Prentice Hall Press; 2011. P. 255–333, 751–831.
8. Wang Y., Lang L., Lee C.H., Zhang B., Chong Y. Topologically enhanced harmonic generation in a nonlinear transmission line metamaterial. *Nat. Commun*. 2019;10:Article number:1102. https://doi.org/10.1038/s41467-019-08966-9
9. Guarcello C., Ahrens F., Avallone G., et al. Nonlinear Behavior of Josephson Traveling Wave Parametric Amplifiers. *IEEE Transactions on Applied Superconductivity*. 2024;34(3):1–5. https://doi.org/10.1109/TASC.2024.3367615
10. Hong M., Chang Y.H., Dienes A., Delfyett P., Dijaili S., Patterson F. Femtosecond self- and cross-phase modulation in semiconductor laser amplifiers. *IEEE Journal of Selected Topics in Quantum Electronics*. 1996;2(3):523–539. https://doi.org/10.1109/2944.571753
11. Hussain S., Siddiqui H., Saleem A., et al. Therapeutic Exercise Recognition Using a Single UWB Radar with AI-Driven Feature Fusion and ML Techniques in a Real Environment. *Sensors*. 2024;24(17):5533. https://doi.org/10.3390/s24175533
12. Oppermann I., Hämäläinen M., Iinatti J. *UWB Theory and Applications*. John Wiley & Sons; 2004, 248 p.
13. Taylor J.D. (Ed.). *Advanced Ultrawideband Radar. Signals, Targets, and Applications.* CRC Press; 2016, 494 p.
14. Bulygin D.A., Mamonova T.E. Recognition of hand gestures in real time. *Sistemy analiza i obrabotki dannykh = Analysis and Data Processing Systems.* 2020;78(1):25–40 (in Russ.). https://doi.org/10.17212/1814-1196-2020-1-25-40
15. Shadinov S.S. Spatial ultra-wideband visualization of probed near-field surveillance objects. *Zhurnal Radioelektroniki = J. Radio Electronics*. 2020;7 (in Russ.). https://doi.org/10.30898/1684-1719.2020.7.8. Available from URL: http://jre.cplire.ru/jre/jul20/8/text.pdf. Accessed May 02, 2026.
16. Wang X., Dinh A., Teng D. Radar Sensing Using Ultra Wideband – Design and Implementation. In: Matin M.A. (Ed.). *Ultra Wideband – Current Status and Future Trends*. 2013;11:41–63. https://doi.org/10.5772/48587
17. Latyshev K.V. Cyberphysical radio-gestural FPV control drones. In: *Actual Problems and Prospects of Development of Radio Engineering and Information Communication systems* (*Radioinfocom – 2024*): *Proceedings of the 8th International Scientific and Practical Conference*. Moscow: RTU MIREA; 2024. P. 441–445 (in Russ.). https://www.elibrary.ru/dukcnp

СПИСОК ЛИТЕРАТУРЫ

1. Khan I., Kwon Y. Radar-based Hand Gesture Recognition with Feature Fusion using Robust CNN-LSTM and Attention Architecture. *IEEE Access*. 2025;13:69281–69291. https://doi.org/10.1109/ACCESS.2025.3558293
2. Костин М.С., Бойков К.А. Цифровые технологии сигнального радиовидения и радиомониторинга. *Russian Technological Journal*. 2024;12(4):59–69. https://doi.org/10.32362/2500-316X-2024-12-4-59-69
3. Wu M. Gesture Recognition Based on Deep Learning: A Review. *EAI Endorsed Transactions on e-Learning*. 2024;10. https://doi.org/10.4108/eetel.5191
4. Qu C., Zhang Y., Jin L., et al. Exploring hand gesture recognition using micro-Doppler radar data based on vision transformers. *J. Phys.: Conf Ser*. 2023;2504:012046. https://doi.org/10.1088/1742-6596/2504/1/012046
5. Sedra A., Smith K., Carusone T., Gaudet V. *Microelectronic Circuits* (*The Oxford Series in Electrical and Computer Engineering*). 8th ed. Oxford University Press; 2020. P. 58–134, 174–246, 508–696.
6. He F., Ribas R., Lahuec C., Jézéquel M. Discussion on the general oscillation startup condition and the Barkhausen criterion. *Analog Integr. Circ. Signal Process*. 2009;59:215–221. https://doi.org/10.1007/S10470-008-9250-1
7. Razavi B. *RF Microelectronics* (*Prentice Hall Communications Engineering and Emerging Technologies Series*). 2nd ed. Prentice Hall Press; 2011. P. 255–333, 751–831.
8. Wang Y., Lang L., Lee C.H., Zhang B., Chong Y. Topologically enhanced harmonic generation in a nonlinear transmission line metamaterial. *Nat. Commun*. 2019;10:Article number:1102. https://doi.org/10.1038/s41467-019-08966-9
9. Guarcello C., Ahrens F., Avallone G., et al. Nonlinear Behavior of Josephson Traveling Wave Parametric Amplifiers. *IEEE Transactions on Applied Superconductivity*. 2024;34(3):1–5. https://doi.org/10.1109/TASC.2024.3367615
10. Hong M., Chang Y.H., Dienes A., Delfyett P., Dijaili S., Patterson F. Femtosecond self- and cross-phase modulation in semiconductor laser amplifiers. *IEEE Journal of Selected Topics in Quantum Electronics*. 1996;2(3):523–539. https://doi.org/10.1109/2944.571753
11. Hussain S., Siddiqui H., Saleem A., et al. Therapeutic Exercise Recognition Using a Single UWB Radar with AI-Driven Feature Fusion and ML Techniques in a Real Environment. *Sensors*. 2024;24(17):5533. https://doi.org/10.3390/s24175533
12. Oppermann I., Hämäläinen M., Iinatti J. *UWB Theory and Applications*. John Wiley & Sons; 2004, 248 p.
13. Taylor J.D. (Ed.). *Advanced Ultrawideband Radar. Signals, Targets, and Applications.* CRC Press; 2016, 494 p.
14. Булыгин Д.А., Мамонова Т.Е. Распознавание жестов рук в режиме реального времени. *Системы анализа и обработки данных.* 2020;78(1):25–40. https://doi.org/10.17212/1814-1196-2020-1-25-40
15. Шадинов С.С. Пространственная сверхширокополосная визуализация зондируемых объектов ближнего радионаблюдения. *Журнал радиоэлектроники*. 2020;7. https://doi.org/10.30898/1684-1719.2020.7.8. URL: http://jre.cplire.ru/jre/jul20/8/text.pdf. Дата обращения 05.02.2026.
16. Wang X., Dinh A., Teng D. Radar Sensing Using Ultra Wideband – Design and Implementation. In: Matin M.A. (Ed.). *Ultra Wideband – Current Status and Future Trends*. 2013;11:41–63. https://doi.org/10.5772/48587

17. Латышев К.В. Киберфизическое радиожестикуляционное FPV-управление дронами. В сб.: *Актуальные проблемы и перспективы развития радиотехнических и инфокоммуникационных систем* («*Радиоинфоком – 2024*»): *Сборник научных статей по материалам VIII Международной научно-практической конференции.* М.: РТУ МИРЭА; 2024. С. 441–445. https://www.elibrary.ru/dukcnp

About the Authors

Kirill V. Latyshev, Senior Lecturer, Department of Radio Wave Processes and Technologies, Institute of Radio Electronics and Informatics, MIREA – Russian Technological University (78, Vernadskogo pr., Moscow, 119454 Russia). E-mail: latyshev@mirea.ru. RSCI SPIN-code 7415-5362, https://orcid.org/0009-0007-4393-6887

Mihail S. Kostin, Dr. Sci. (Eng.), Associate Professor, Head of the Department of Radio Wave Processes and Technologies, Deputy Director, Institute of Radio Electronics and Informatics, MIREA – Russian Technological University (78, Vernadskogo pr., Moscow, 119454 Russia). E-mail: kostin_m@mirea.ru. Scopus Author ID 57208434671, RSCI SPIN-code 5819-2178, http://orcid.org/0000-0002-5232-5478

Konstantin A. Boikov, Dr. Sci. (Eng.), Professor, Department of Radio Wave Processes and Technologies, Institute of Radio Electronics and Informatics, MIREA – Russian Technological University (78, Vernadskogo pr., Moscow, 119454 Russia). E-mail: boykov@mirea.ru. Scopus Author ID 57208926258, RSCI SPIN-code 2014-6951, http://orcid.org/0000-0003-0213-7337

Об авторах

Латышев Кирилл Валерьевич, старший преподаватель, кафедра радиоволновых процессов и технологий, Институт радиоэлектроники и информатики, ФГБОУ ВО «МИРЭА – Российский технологический университет» (119454, Россия, Москва, пр-т Вернадского, д. 78). E-mail: latyshev@mirea.ru. SPIN-код РИНЦ 7415-5362, https://orcid.org/0009-0007-4393-6887

Костин Михаил Сергеевич, д.т.н., доцент, заведующий кафедрой радиоволновых процессов и технологий, заместитель директора Института радиоэлектроники и информатики, ФГБОУ ВО «МИРЭА – Российский технологический университет» (119454, Россия, Москва, пр-т Вернадского, д. 78). E-mail: kostin_m@mirea.ru. Scopus Author ID 57208434671, SPIN-код РИНЦ 5819-2178, http://orcid.org/0000-0002-5232-5478

Бойков Константин Анатольевич, д.т.н., профессор, кафедра радиоволновых процессов и технологий, Институт радиоэлектроники и информатики ФГБОУ ВО «МИРЭА – Российский технологический университет» (119454, Россия, Москва, пр-т Вернадского, д. 78). E-mail: boykov@mirea.ru. Scopus Author ID 57208926258, SPIN-код РИНЦ 2014-6951, http://orcid.org/0000-0003-0213-7337

Translated from Russian into English by Kirill V. Nazarov
Edited for English language and spelling by Dr. David Mossop